Carbon-13 Chemical-Shift Tensors in Polycyclic Aromatic Compounds. 9.[1] Biphenylene

Dewey H. Barich, Anita M. Orendt, Ronald J. Pugmire,[†] and David M. Grant*

Departments of Chemistry and Chemical and Fuels Engineering, University of Utah, Salt Lake City, UT, 84112

Received: May 25, 2000

The principal values of the ^{13}C chemical-shift tensors of natural abundance biphenylene were measured at room temperature with the FIREMAT experiment. Of 18 crystallographically distinct positions (three sets of six congruent carbons each), the three primary bands have been resolved into seven single peaks and four degenerate peaks (two double, one triple, and one quadruple). Hence, eleven different chemical-shift tensors are reported. An interpretation of the data is made by comparison to carbon chemical-shift tensors in other molecules with similar chemical environments. Experimental and theoretical values based on a model of the asymmetric unit of the crystal unit cell are in good agreement.

Introduction

The measurement of ^{13}C chemical-shift tensors of polycyclic aromatic hydrocarbons has received considerable attention in recent years.[1−4] Challenges to measuring chemical-shift tensors in aromatic microcrystalline powders include the complexity of the spectrum due to the spinning sideband patterns, the relatively close isotropic chemical shifts of the various carbons in the molecule (typically from 120 to 140 ppm), and the extensive overlap of molecularly equivalent peaks from crystallographically inequivalent positions. The complexity of these spectra may be reduced by employing a two-dimensional (2D) magic angle turning (MAT) experiment that isolates individual sideband patterns associated with different isotropic chemical shifts from the composite spectrum. Recent advances in such methods have made possible the isolation of several dozen sideband patterns from a complicated spectrum.[5−7] Prior to the development of the FIREMAT experiment (FIREMAT stands for *fi*ve-*π re*plicated *MAT*), the spectrum of biphenylene would have been too complicated to obtain well-resolved spectra, largely due to coincidental degeneracy of nearly overlapping isotropic shifts that arise from similar molecular positions found in different crystallographic positions. The FIREMAT experiment separates individual spinning sideband patterns by identifying them with their respective isotropic chemical shifts. An isotropic chemical shift spectrum is extracted from the pseudo-2D data. Hence, a sideband pattern can be extracted for each resolvable isotropic chemical shift. At first glance, one would expect to find only three peaks in the biphenylene crystal system, one for each molecular position; however, the crystal system has eighteen inequivalent carbon positions. The fact that the three molecular positions of biphenylene are further resolved in the crystal system (due to magnetic inequivalencies in the crystallographic space group) demonstrates the potential advantages of solid-state NMR.

There are six biphenylene molecules present in a total of four asymmetric units in the *P*2₁/a unit cell,[8] and they exhibit two different biphenylene structures present in a 1:2 ratio. The minor structure labeled P (with two molecules per unit cell) is planar while the major structure (with four molecules per unit cell) labeled D, deviates very slightly from planarity. Thus, there is one entire biphenylene molecule D and half of a biphenylene molecule P in each asymmetric unit, resulting in eighteen

inequivalent NMR carbon environments in the crystal. The eighteen lines group into three sets of six closely positioned congruent carbon bands with some lines resolved in each set. In this work, the FIREMAT experiment[7] isolated 11 sideband patterns in the biphenylene crystal system, one for each resolved isotropic chemical shift in the spectrum (Figure 1).

Biphenylene is an interesting model compound in the study of ^{13}C chemical-shift tensors due to its strained central ring.[9−11] The detailed relationship between ring strain and the chemical-shift tensor principal values, while incompletely understood, is of fundamental interest. In a pragmatic sense biphenylene is a possible component in carbonaceous materials such as coal and soot.[12] Hence, the chemical-shift tensors of biphenylene make an important contribution to the study of complex carbonaceous materials important to industry and the environment.

Biphenylene has also been used as a model compound in the study of antiaromaticity,[13−15] as this fused aromatic molecule is the dibenzo derivative of cyclobutadiene, a classic example of antiaromaticity that is difficult to study due to thermal instability. The four-membered ring of biphenylene contains four π-electrons, thus satisfying Hückel's rule[16] for an antiaromatic ring. Hückel's rule predicts that a *monocyclic* polyene with ($4n + 2$) π electrons will be more stable than the corresponding acyclic analogue because of a degeneracy in the lowest energy state. Conversely, if there are only $4n$ π-electrons in the monocyclic polyene, the molecule will be less stable than the acyclic analogue. Such molecules are called antiaromatic. The antiaromaticity of the central ring of biphenylene has been determined through a variety of methods. Among them is Schleyer's Nucleus Independent Chemical Shift (NICS) scheme,[17] which has been applied to numerous molecules.[18−20] The NICS scheme is a criterion for determining aromatic and antiaromatic character in which one evaluates the isotropic chemical shift at the nonweighted geometric center of a ring by calculating the chemical shielding at that location and changing its sign. The change in sign aligns the *direction* of the NICS and the experimental chemical shift scales, although they still have different zero points. The NICS value is then interpreted as aromatic (negative) or antiaromatic (positive) depending upon the sign of the NICS shift. While the central four-member ring of biphenylene has antiaromatic character, the two six-membered

[13]C Chemical-Shift Tensors

J. Phys. Chem. A, Vol. 104, No. 35, 2000 **8291**
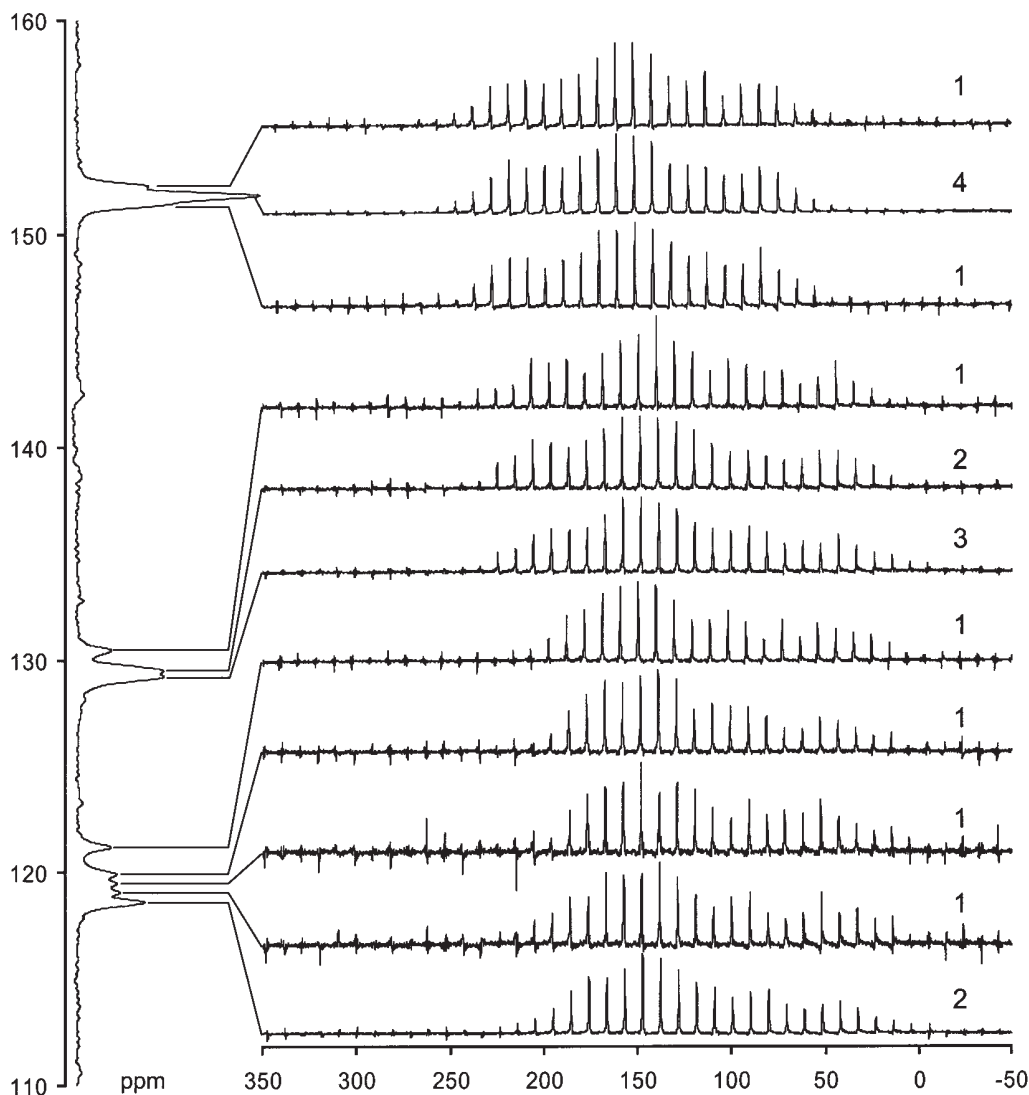
Figure 1. FIREMAT ^{13}C spectra for natural abundance biphenylene. All spectra were derived from one FIREMAT dataset. See text for details. The numbers listed on the right side of the figure indicate the approximate relative intensity of each spectrum.

rings are markedly aromatic in character, which contributes to the stability of the molecule.

Comparison with previously determined ^{13}C chemical-shift tensors of some chemical environments similar to biphenylene is made to better understand the chemical-shift tensors in strained molecules. Comparison of measured chemical-shift tensors to those calculated at several levels of theory was also made to rationalize the assignment of the chemical-shift tensors to individual crystallographic positions of congruent carbons.

Methods

Experimental. Biphenylene was purchased from Aldrich and used without further purification. The crystalline form was verified by comparing an X-ray diffraction spectrum to a simulated spectrum based on the literature crystal structure.[8] All NMR experiments were carried out on a CMX-200 NMR spectrometer with a [13]C Larmor frequency of 50.307 MHz. The [1]H T_1 of the sample was determined by saturation recovery to be approximately 69 s at a ^{1}H frequency of 200.0 MHz. To enhance signal intensity, cross polarization[21] was used with an optimal contact time of 2.5 ms. Proton decoupling was carried out at a field strength of approximately 61.0 kHz. A FIREMAT experiment[7] was carried out on the sample. With use of a flip-

back pulse, the optimum recycle delay was 60 s. A total of 384 scans were collected in each of the eight evolution points so that the entire experiment time was slightly more than 2 days. In the FIREMAT experiment, the sample spinning speed was 480 Hz. The spectral width in the acquisition and evolution dimensions were 23 040 and 3840 Hz, respectively. Data were transferred to a Sun computer for processing and spectral analysis. TIGER processing[6] of the pseudo-2D data generated an isotropic guide FID that was then fit as the sum of eleven model FIDs. The resulting model was used to extract the FIDs for each of the resolved spinning sideband patterns that were then fit to yield principal values for the chemical-shift tensors.

Theoretical. To simulate the spectra of crystallographically inequivalent carbons in the experimental portion of this work, a faithful model is needed that captures the degeneracies common to congruent carbons in the crystallographic asymmetric unit. The smallest practical model is one in which the asymmetric unit is augmented with the remainder of the fragmented biphenylene molecule, thus forming a two-molecule asymmetric unit model (AUM). The level of theory used to calculate the chemical-shift tensors for the AUM was selected by performing a series of calculations on a single molecule of biphenylene.

In the single molecule model (SMM), a partial optimization was carried out at the B3PW91 level of theory[22] with Dunning's cc-pVDZ basis set[23] on molecule D from the asymmetric unit. Keeping the carbon nuclei in their crystallographic positions, only the proton positions were optimized with Gaussian 98.[24] Chemical-shift tensors were calculated for the SMM at the RHF,[25] MP2,[26,27] B3LYP,[28,29] and B3PW91 levels of theory. The shielding calculation on the AUM was performed at the B3PW91 level of theory. All shielding calculations employed the GIAO ansatz.[30] One shielding calculation was carried out on the SMM at the B3PW91 level of theory with the cc-pVTZ basis set. All other shielding calculations employed the cc-pVDZ basis set.[23] The principal values from the B3PW91/cc-pVTZ calculation were compared against those from the B3PW91/cc-pVDZ to demonstrate the correspondence between the calculated shieldings with each of these basis sets. For each of the four cc-pVDZ calculations on the SMM, the calculated principal shielding values were plotted against the experimental shift values. The linear regression performed on each plot was then used to correlate the calculated chemical shieldings to chemical shifts.

The AUM was partially optimized in the same fashion as SMM above. A single chemical shift calculation was carried out on AUM at the B3PW91/cc-pVDZ level of theory based on the chemical-shift tensor results of the SMM for both the choice of level of theory and the choice of basis set. Calculated chemical shieldings were correlated to the chemical shift scale in the same fashion as above.

Results and Discussion

Figure 1 contains the FIREMAT experiment spectra. The possibility that some of the lines were due to polymorphs of biphenylene was ruled out by comparing the X-ray diffraction to a simulation of a diffraction spectrum based on the crystal structure. Instead, the lines are due to the eighteen magnetically inequivalent carbons in the asymmetric unit.

The guide spectrum, exhibiting 11 unique lines, was extracted from the pseudo-2D data and is displayed on the left of the figure. The guide spectrum is an isotropic chemical shift spectrum which is fully equivalent to a high-speed MAS spectrum but is obtained from the pseudo-2D data as described previously.[7] The guide spectrum has approximately 1:1:1 integrated bands for each of the three subsets of carbons (quaternary, α, and β positions), although each region is partially resolved further due to minor intermolecular interactions arising from the different crystallographic positions. In the quaternary position ($\delta_{iso} \approx 150$ ppm) there are three resolved lines in a 1:4:1 ratio. The middle line exhibits a 4-fold degeneracy. For the α position ($\delta_{iso} \approx 120$ ppm) there are five lines, the most upfield of which has double intensity due to accidental degeneracy of these two isotropic chemical shifts. The β position ($\delta_{iso} \approx 130$ ppm) shows three resolved peaks with weighting degeneracies of 1:2:3. While indeterminable, the extent of accidental or near degeneracy in this subset is of minor consequence as the data indicate that all of the principal values lie within the experimental error. Note, the inability to show that two or more tensors differ from one another is not a failure to measure the overlapping tensors. Admittedly, degenerate peaks cannot be assigned to specific carbons, but their identification with congruent sites is straightforward.

Table 1 contains the chemical-shift tensor principal values of biphenylene determined with the FIREMAT experiment. Also included are the span (Ω) and acentricity ($\kappa\Omega/3$), all the components of which are defined elsewhere.[31] Assignment of

TABLE 1: Measured ^{13}C Chemical-Shift Tensors of Biphenylene

carbon[a]	δ_{11} ppm	δ_{22} ppm	δ_{33} ppm	δ_{iso} ppm	span ppm	acentricity ppm
Q	245.8	156.9	54.1	152.3	191.7	6.986
Q	245.7	155.3	54.3	151.8	191.3	5.292
Q	245.3	153.1	55.7	151.4	189.7	2.633
β	227.6	145.7	18.1	130.5	209.6	22.830
β	229.9	146.2	12.6	129.6	217.3	24.931
β	227.2	146.6	13.8	129.2	213.5	26.133
α	199.6	150.7	13.3	121.2	186.3	44.298
α	198.2	146.4	15.3	120.0	182.9	39.605
α	196.3	146.0	16.2	119.5	180.1	39.791
α	202.0	144.8	10.4	119.1	191.6	38.598
α	199.6	144.4	11.8	118.6	187.9	38.697

[a] Each carbon is labeled according to its molecular position as quaternary, α, or β.

the isotropic peaks to quaternary, α, or β positions is simple given their relatively large separation and correspondence to previous solution assignments.[32] The calculated values (vide infra) confirm this general grouping of lines. Assignment of the measured tensors to the crystallographic positions was investigated by calculating the variance between the calculated and experimental principle values for all 720 possible permutations of the assignments within each of the molecular positions (quaternary, α, or β) and applying the F-test to see if any one assignment was significantly better than another. Hence, the assignments contained in this work are those with the best least-squares fit. Unfortunately, statistics fail to demonstrate that this assignment is superior to at least some of the other possibilities because the tensors between corresponding crystallographic positions tend to be degenerate.

Quaternary Chemical-shift Tensors. It is interesting to compare the chemical-shift tensors of the biphenylene molecule, **1**, with similar unusual structures. One notable case is cyclobutadiene, **2**, of which biphenylene is the dibenzo derivative. Both **2** and the center ring of **1** are antiaromatic. Each satisfies Hückel's rule for molecules having $4n$ π electrons ($n = 1$) in a monocyclic polyene ring and exhibit positive chemical shifts in the NICS scheme (vide supra).
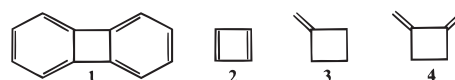

The ^{13}C chemical-shift tensor of **2** has principal values of 267, 92, and 78 ppm.[33] These values reflect the ring strain present in the cyclobutadiene ring. The δ_{33} component, which best reflects the effects of ring strain (vide infra), is considerably downfield ($\Delta\delta = 24$ ppm) compared to 54 ppm, the δ_{33} component for the quaternary position in **1**. The chemical-shift tensors for the quaternary position are not like the condensed position in naphthalene (cf. 208, 202, −6 ppm).[34] Instead, the chemical-shift tensors here appear more like a substituted carbon position, as was found in previous work on triphenylene[2] in which the C−C bonds connecting any two rings have virtually no π character. The same appears to be the case for biphenylene; the average C−C distance between two quaternary carbons in different rings is slightly greater than 1.51 Å in biphenylene, a bond length quite typical of a C−C single bond. The difference in the values between **1** and **2** reflects the increased stability of **1**.

Orendt et al.[35] reported the ^{13}C chemical-shift tensors of a number of olefinic compounds, several of which have four-membered rings that provide comparable tensors. These include

[13]C Chemical-Shift Tensors

*J. Phys. Chem. A, Vol. 104, No. 35, 2000* **8293**

methylenecyclobutane, **3**, and 1,2-bis(methylene)cyclobutane, **4**. The δ_{11} principal values of the chemical-shift tensor for the quaternary positions in **1** (ca. 246 ppm) are consistent with values for other quaternary positions with carbon substituents that possess double-bond character in the *exo*-CH_2 double bond attached to the ring in **3** or **4** (253 and 250 ppm, respectively). The δ_{11} value of the $=CH_2$ carbon in **4** is more similar to **1**, probably due to the similar conjugation in **1** and **4**. There is also similarity in the δ_{33} components not only for the molecules mentioned above but also for other four-member ring systems, particularly those which are substituted to any degree. These include 1,2-dimethylcyclobutene, bicyclo[2.2.0]hex-1(4)-ene, bicyclo[3.2.0]hept-1(5)-ene, and bicyclo[4.2.0]hept-1(6)-ene with δ_{33} components of 45, 46, 56, and 43 ppm, respectively. The common occurrence of this downfield shift of the δ_{33} component in these four-member rings suggests that it is due primarily to ring strain. Note, δ_{33} appear in the range of $10-20$ ppm for typical six-member rings.[36] This is consistent with chemical-shift tensor data recently reported by Orendt et al.[1] for coronene and corannulene.

Chemical-Shift Tensors of Protonated Carbons. The protonated carbons exhibit more conventional aromatic C−H tensor values. The α positions have isotropic chemical shifts which are shifted upfield from typical aromatic positions by ca. 8 ppm. This upfield shift is almost entirely due to the δ_{11} component which is upfield compared to other typical aromatic systems. This can be rationalized in terms of the relatively greater electron shielding at the α position due to the preference for the resonance structure with a double bond between the quaternary and α positions. This is also supported by the relative lengths of the carbon−carbon bonds in the diffraction structures. The isotropic chemical shifts of the β positions are only modestly upfield from that of benzene at cryogenic temperatures.[37−39] The chemical-shift tensor principal values for the β positions are quite similar to the analogous positions in naphthalene, viz., 228, 139, and 11 ppm.[34]

Calculated Tensors. The partial optimizations of the SMM and the AUM resulted in C−H distances in both structures which are very similar to the average C−H distance reported in an electron diffraction study of biphenylene (1.096 ± 0.009 Å).[40] Figure 2 shows a plot of the B3LYP/cc-pVTZ principal values plotted against the B3LYP/cc-pVDZ principal values. There is a high degree of correlation between the two sets of calculated data. The use of the double-ζ instead of triple-ζ basis set therefore differs primarily only in terms of the actual values for the slope and intercept; both have comparable correlation coefficients and rms measures. The triple-ζ slope exceeds unity by almost the same amount as the double-ζ underestimates the correlation slope. The two levels of approximation at the B3PW91 level of theory thus have comparable merit. This correlation approach for converting calculated shieldings to the experimental shift scale has succeeded in a number of efforts[2−4,41−45] in this lab. The linear relationship between the values calculated with cc-pVDZ and cc-pVTZ justifies the use of the smaller basis set for the calculation on the larger AUM because the calculated values are correlated to the experimental scale by means of a linear regression. In many chemical shift calculations in the literature the conversion of calculated shieldings to the chemical shift scale is achieved by calculating the difference between the shielding of TMS (or some secondary reference) and the value of interest.[46,47] It is well established that in these cases it is necessary to use basis sets of at least triple-ζ quality to obtain accurate results.[48] The correlation approach used in this laboratory negates these minor problems
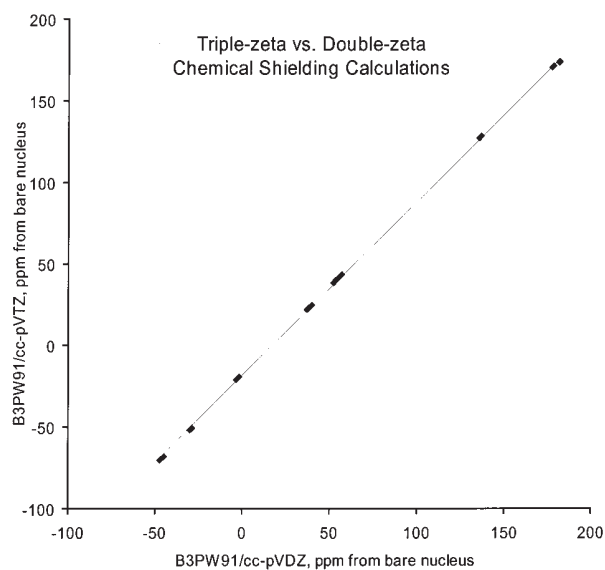

Figure 2. Plot of the shielding principal values for biphenylene calculated at the B3LYP level of theory with the cc-pVTZ basis set vs those calculated at the same level of theory with the cc-pVDZ basis set for the SMM. The high correlation ($\sigma^2 = 0.9998$ and rms = 1.17 ppm) between the two approaches demonstrates the validity of using the smaller basis set to correlate calculated and measured data.
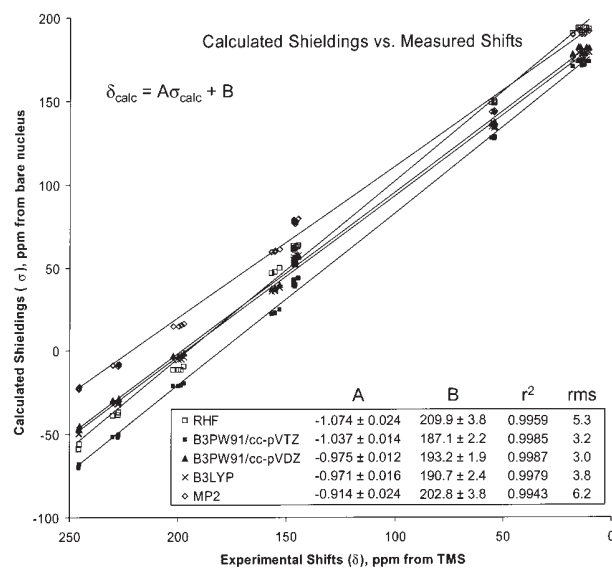
Figure 3. Plot of the calculated vs experimental principal values for the SMM used to select the level of theory to calculate the chemical-shift tensors for the AUM. The linear regression equation for each level of theory is included with uncertainties provided at the 95% confidence interval. These equations were used to correlate the calculated values to the experimental scale as described in the text.

and avoids the need to calculate the shielding of a reference compound that has considerable differences in electronic structure. It also has the desirable property of improving any statistical analysis between the converted calculated values and the measured values because the use of the correlation equation should eliminate any systematic errors, thus leaving (in principle) only random errors. It is important to note that this approach is not always feasible when there are an insufficient number of experimental values to reliably correlate the experimental and calculated values. Solid-state NMR studies have an advantage over gas or solution phase studies in this regard in that there are three principal values available from the solid-

8294 *J. Phys. Chem. A, Vol. 104, No. 35, 2000*

Barich et al.
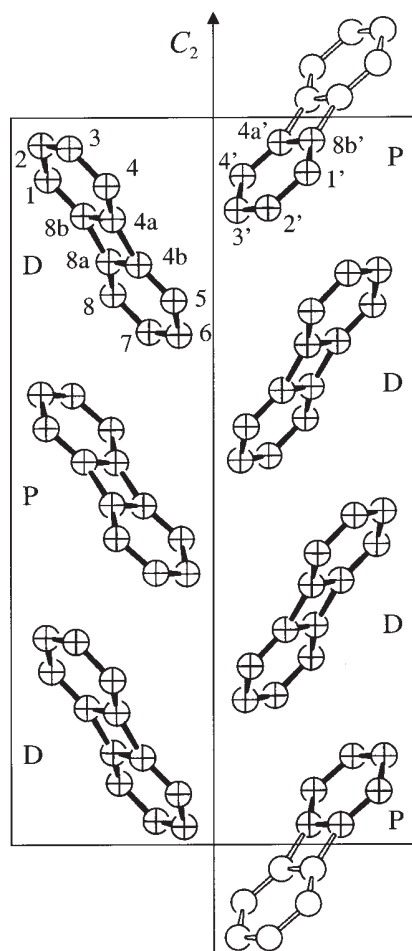
Figure 4. Simplified representation showing those molecules associated with one biphenylene unit cell. The effect of the 2-fold screw axis is most easily understood by following the planar (P) molecules (which contain an inversion center) through the screw axis operation. The P molecule near the bottom right of the image is rotated about the C_2 axis and is then translated up the axis by one-half of that direction's unit cell length to locate the one P molecule shown on the left side of the axis. Repetition of that operation identifies the P molecule near the upper right corner of the figure. The two sites occupied by the distorted (D) molecules are repeated similarly. One-half of each of the two P molecules on the right side of the figure lie outside the unit cell boundaries which is emphasized by the removal of their hatch patterns present on all carbons that lie inside the boundaries. The labels for the top 18 carbons which lie inside the boundary correspond to the calculated tensors in Table 2.

state experiment for each nucleus under study compared with single isotropic values in gas or solution studies.

For the SMM, once the calculated shielding tensors were correlated to the experimental chemical-shift tensors by the regression equations shown in Figure 3, the root-mean-square (rms) deviations between the calculated principal values of the SMM and the measured principal values were calculated. The RHF and MP2 rms deviations were 5.3 and 6.2 ppm, respectively. The B3LYP and B3PW91 (cc-pVDZ and cc-pVTZ) shift calculations had rms deviations in ppm of 3.8, 3.0, and 3.2, respectively. These rms deviations for the DFT methods are comparable to other aromatic hydrocarbon work in this laboratory.[1,2,49]

Figure 4 shows a representation of the biphenylene crystal. The AUM used for the chemical-shift calculations consists of the topmost molecule P and molecule D in the figure (including the half of molecule P in the upper right corner that had its

TABLE 2: Calculated ^{13}C Chemical-Shift Tensors of Biphenylene

carbon[a] ppm	number ppm	δ_{11} ppm	δ_{22} ppm	δ_{33} ppm	δ_{iso} ppm	span ppm	acentricity ppm
Q	8b	246.6	161.2	57.2	155.0	189.4	9.297
Q	4b	246.7	159.8	58.3	154.9	188.4	7.319
Q	8a	246.6	159.3	57.9	154.6	188.7	7.059
Q	4a′	244.8	158.2	57.5	153.5	187.3	7.023
Q	4a	245.1	158.6	56.5	153.4	188.6	7.735
Q	8b′	244.6	157.2	58.4	153.4	186.2	5.707
α	3′	227.7	148.2	12.5	129.5	215.3	28.086
α	3	229.7	144.2	14.0	129.3	215.7	22.316
α	2	229.1	144.6	14.2	129.3	214.9	22.967
α	2′	230.2	142.4	14.9	129.2	215.3	19.848
α	6	228.0	144.4	13.8	128.7	214.2	23.527
α	7	228.0	142.8	14.5	128.4	213.5	21.611
β	1′	201.9	141.8	11.8	118.5	190.1	34.995
β	4	202.0	143.2	9.6	118.3	192.4	37.443
β	5	202.7	140.5	11.5	118.2	191.2	33.320
β	8	201.3	141.2	11.2	117.9	190.1	34.939
β	4′	201.0	140.6	11.2	117.6	189.8	34.491
β	1	200.9	139.4	10.9	117.1	190.1	33.522

^{a} Each carbon is labeled according to its molecular position as quaternary, α, or β.

hatch pattern removed). While all twelve carbons in molecule P were included in the calculations, only the six hatched carbons which lie inside the boundary box in the figure were reported and used in the data correlations with experiment. The eighteen carbons involved in the data analysis (twelve from molecule D and 6 from molecule P) represent the asymmetric unit of the biphenylene crystal.

As above in the SMM, the 18 calculated chemical shieldings associated with the asymmetric unit from the AUM were correlated to the experimental scale via a linear regression of the form $\delta_{calc} = -0.9768 \ (\pm0.0102) \ \sigma_{calc} + 193.4 \ (\pm1.6)$. Uncertainties are provided in parentheses at the 95% confidence level. The rms differences for these calculated values are 1.0 ppm for the isotropic values and 3.1 ppm for the principal values. Table 2 contains the chemical-shift tensors, spans, and acentricities for the AUM calculated at the B3PW91/cc-pVDZ level of theory.

While the calculated tensors are in very good overall agreement with the experimental values, the δ_{22} components of the α and β positions were outliers relative to the overall regression in SMM, particularly at the RHF and MP2 levels of theory (see Figure 3). There is considerable improvement in the δ_{22} principal components for the calculations in which the chemical-shift tensors were calculated with DFT. The shortcomings appearing at the RHF and MP2 levels are not unduly surprising. RHF theory does not treat electron correlation, and the MP2 level of theory is only the first step in a perturbative series and is generally believed to overcompensate the estimates of electron correlation.[50,51] The use of the semi-empirical DFT methods appears to offer a better approximation of the effects of charge densities and electron correlation and provides improved results over both the RHF and MP2 calculations. This is demonstrated in a quantitative fashion by inspecting the regression equations for SMM shown in Figure 3. In this work, all of the DFT approaches exhibited regression slopes much closer to the idealized case of -1 than either the RHF or the MP2 results. The regression intercepts for the DFT methods are also improved over the RHF and MP2 methods, having values nearer the idealized case of the estimated 185.4 ppm shielding value of TMS.[52] The uncertainties in both the slopes and intercepts are nearly a factor of 2 smaller than the respective

¹³C Chemical-Shift Tensors

J. Phys. Chem. A, Vol. 104, No. 35, 2000 **8295**

values for the RHF and MP2 methods (see Figure 3 for 95% confidence limits).

Conclusions

Interpretation and analysis of complicated solid state NMR spectra are more easily facilitated by use of 2D experiments. The principal values for the chemical-shift tensor of the quaternary carbons in biphenylene reflect the ring strain of the four-membered ring. This suggests that the quaternary position is chemically similar to a substituted aromatic position, and not to a conjugated aromatic bridgehead carbon such as that found in naphthalene. The effects of ring strain are most clearly apparent in the δ_{33} component of the chemical-shift tensor. The use of double-ζ basis sets instead of triple-ζ basis sets is justified on the basis of computational simplicity and the monotonic linear relationship between calculations with a triple-ζ basis set and a double-ζ basis set. All of the calculated chemical-shift tensors show good correlation with experimental values, but those calculated with DFT are particularly good in calculating the shift magnitudes between the various spectral peaks. This latter agreement is tentatively attributed to better effective treatment of electron correlation in the semiempirical DFT methods.

References and Notes

(1) Previous paper in this series: Orendt, A. M.; Facelli, J. C.; Bai, S.; Rai, A.; Gossett, M.; Scott, L. T.; Boerio-Goates, J.; Pugmire, R. J.; Grant, D. M. *J. Phys. Chem. A* **2000**, *104*, 149−155.
(2) Iuliucci, R. J.; Phung, C. G.; Facelli, J. C.; Grant, D. M. *J. Am. Chem. Soc.* **1998**, *120*, 9305−9311.
(3) Iuliucci, R. J.; Phung, C. G.; Facelli, J. C.; Grant, D. M. *J. Am. Chem. Soc.* **1996**, *118*, 4880−4888.
(4) Iuliucci, R. J.; Facelli, J. C.; Alderman, D. W.; Grant, D. M. *J. Am. Chem. Soc.* **1995**, *117*, 2336−2343.
(5) Gan, Z. *J. Am. Chem. Soc.* **1992**, *114*, 8307−8309.
(6) McGeorge, G.; Hu, J. Z.; Mayne, C. L.; Alderman, D. W.; Pugmire, R. J.; Grant, D. M. *J. Magn. Reson.* **1997**, *129*, 134−144.
(7) Alderman, D. W.; McGeorge, G.; Hu, J. Z.; Pugmire, R. J.; Grant, D. M. *Mol. Phys.* **1998**, *95*, 1113−1126.
(8) Fawcett, J. K.; Trotter, J. *Acta Crystallogr.* **1966**, *20*, 87−93.
(9) Kovaček, D.; Margetić, D.; Maksić, Z. B. *J. Mol. Struct. (THEOCHEM)* **1993**, *285*, 195−210.
(10) Maksić, Z. B.; Kovaček, D.; Eckert-Maksić, M.; Böckmann, M.; Klessinger, M. *J. Phys. Chem.* **1995**, *99*, 6410−6416.
(11) Eckert-Maksić, M.; Fabian, W. M. F.; Janoschek, R.; Maksić, Z. B. *J. Mol. Struct. (THEOCHEM)* **1995**, *338*, 1−10.
(12) Muñoz, R. H.; Charalampopoulos, T. T., *Twenty-seventh Symposium (International) on Combustion*, The Combustion Institute: Pittsburgh, 1998, pp 1471−1479.
(13) Breslow, R. *Acc. Chem. Res.* **1973**, *6*, 393−398.
(14) Bich, V. T.; Bini, R.; Salvi, P. R. *Chem. Phys. Lett.* **1990**, *175*, 413−418.
(15) Zimmermann, R. *J. Mol. Struct.* **1996**, *377*, 35−46.
(16) Hückel, E. *Z. Phys.* **1931**, *76*, 628−648.
(17) Schleyer, P. v. R.; Maerker, C.; Dransfeld, A., Jiao, H.; Hommes, N. J. R. v. E. *J. Am. Chem. Soc.* **1996**, *118*, 6317−6318.
(18) Fokin, A. A.; Jiao, H.; Schleyer, P. v. R. *J. Am. Chem. Soc.* **1998**, *120*, 9364−9365.

(19) Cossia, F. P.; Morao, I.; Jiao, H.; Schleyer, P. v. R. *J. Am. Chem. Soc.* **1999**, *121*, 6737−6746.
(20) Nyulaszi, L.; Schleyer, P. v. R. *J. Am. Chem. Soc.* **1999**, *121*, 6872−6875.
(21) Pines, A.; Gibby, M. G.; Waugh, J. S. *J. Chem. Phys.* **1973**, *59*, 569−590.
(22) Perdew, J. P.; Wang, Y.; *Phys. Rev. B* **1992**, *45*, 13244−13249.
(23) Dunning, T. H., Jr. *J. Chem. Phys.* **1989**, *90*, 1007−1023.
(24) *Gaussian 98* (Revision A.7); Frisch, M. J.; Trucks, G. W.; Schlegel, H. B.; Scuseria, G. E.; Robb, M. A.; Cheeseman, J. R.; Zakrzewski, V. G.; Montgomery, Jr., J. A.; Stratmann, R. E.; Burant, J. C.; Dapprich, S.; Millam, J. M.; Daniels, A. D.; Kudin, K. N.; Strain, M. C.; Farkas, O.; Tomasi, J.; Barone, V.; Cossi, M.; Cammi, R.; Mennucci, B.; Pomelli, C.; Adamo, C.; Clifford, S.; Ochterski, J.; Petersson, G. A.; Ayala, P. Y.; Cui, Q.; Morokuma, K.; Malick, D. K.; Rabuck, A. D.; Raghavachari, K.; Foresman, J. B.; Cioslowski, J.; Ortiz, J. V.; Baboul, A. G.; Stefanov, B. B.; Liu, G.; Liashenko, A.; Piskorz, P.; Komaromi, I.; Gomperts, R.; Martin, R. L.; Fox, D. J.; Keith, T.; Al-Laham, M. A.; Peng, C. Y.; Nanayakkara, A.; Gonzalez, C.; Challacombe, M.; Gill, P. M. W.; Johnson, B.; Chen, W.; Wong, M. W.; Andres, J. L.; Gonzalez, C.; Head-Gordon, M.; Replogle, E. S.; Pople J. A. Gaussian, Inc.: Pittsburgh, PA, 1998.
(25) Ditchfield, R. *Mol. Phys.* **1974**, *27*, 789−807.
(26) Møller, C.; Plesset, M. S. *Phys. Rev.* **1934**, *46*, 618−622.
(27) Gauss, J. *Chem. Phys. Lett.* **1992**, *191*, 614−620.
(28) Becke, A. D. *J. Chem. Phys.* **1993**, *98*, 5648−5652.
(29) Lee, C.; Yang, W.; Parr, R. G. *Phys. Rev. B* **1988**, *37*, 785−789.
(30) Wolinski, K.; Hinton, J. F.; Pulay, P. *J. Am. Chem. Soc.* **1990**, *112*, 8251−8260.
(31) Mason, J. *Solid State Nucl. Magn. Reson.* **1993**, *2*, 285−288.
(32) Jones, A. J.; Grant, D. M. *Chem. Commun.* **1968**, 1670−1671.
(33) Orendt, A. M.; Arnold, B. R.; Radziszewski, J. G.; Facelli, J. C.; Malsch, K. D.; Strub, H.; Grant, D. M.; Michl, J. *J. Am. Chem. Soc.* **1988**, *110*, 2648−2650.
(34) Sherwood, M. H.; Facelli, J. C.; Alderman, D. W.; Grant, D. M. *J. Am. Chem. Soc.* **1991**, *113*, 750−753.
(35) Orendt, A. M.; Facelli, J. C.; Beeler, A. J.; Reuter, K.; Horton, W. J.; Cutts, P.; Grant, D. M.; Michl, J. *J. Am. Chem. Soc.* **1988**, *110*, 3386−3392.
(36) Orendt, A. M.; Solum, M. S.; Sethi, N. K.; Hughes, C. D.; Pugmire, R. J.; Grant, D. M. In *Advances in Chemistry Series 229*, Botto, R. E.; Sanada Y., Eds.; American Chemical Society: Washington, DC, 1993; pp 419−439.
(37) Pines, A.; Gibby, M. G.; Waugh, J. S. *Chem. Phys. Lett.* **1972**, *15*, 373−376.
(38) Linder, M.; Höhener, Ernst, R. R. *J. Magn. Reson.* **1979**, *35*, 379−386.
(39) Strub, H.; Beeler, A. J.; Grant, D. M.; Michl, J.; Cutts, P. W.; Zilm, K. W. *J. Am. Chem. Soc.* **1983**, *105*, 3333−3334.
(40) Yokozeki, A.; Wilcox, C. F., Jr.; Bauer, S. H. *J. Am. Chem. Soc.* **1974**, *96*, 1026−1032.
(41) Harper, J. K.; McGeorge, G.; Grant, D. M. *J. Am. Chem. Soc.* **1999**, *121*, 6488−6496.
(42) Harper, J. K.; McGeorge, G.; Grant, D. M. *Magn. Reson. Chem.* **1998**, *36*, S135−S144.
(43) Liu, F.; Orendt, A. M.; Alderman, D. W.; Grant, D. M. *J. Am. Chem. Soc.* **1997**, *119*, 8981−8984.
(44) Facelli, J. C.; Orendt, A. M.; Jiang, Y. J.; Pugmire, R. J.; Grant, D. M. *J. Phys. Chem.* **1996**, *100*, 8268−8272.
(45) Anderson-Altmann, K. L.; Phung, C. G.; Mavromoustakos, S.; Zheng, J.; Facelli, J. C.; Poulter, C. D.; Grant, D. M. *J. Phys. Chem.* **1995**, *99*, 10454−10458.
(46) Cheeseman, J. R.; Trucks, G. W.; Keith, T. A.; Frisch, M. J. *J. Chem. Phys.* **1996**, *104*, 5497−5509.
(47) Barich, D. H.; Nicholas, J. B.; Xu, T.; Haw, J. F. *J. Am. Chem. Soc.* **1998**, *120*, 12342−12350.
(48) Sieber, S.; Schleyer, P. v. R.; Gauss, J. *J. Am. Chem. Soc.* **1993**, *115*, 6987−6988.
(49) Orendt, A. M.; Hu, J. Z.; Jiang, Y. J.; Facelli, J. C.; Wang, W.; Pugmire, R. J.; Ye, C.; Grant, D. M. *J. Phys. Chem. A* **1997**, *101*, 9169−9175.
(50) Gauss, J.; *J. Chem. Phys.* **1993**, *99*, 3629−3643.
(51) Gauss, J. *Chem. Phys. Lett.* **1994**, *229*, 198−203.
(52) Jameson, C. J.; Mason, J. In *Multinuclear NMR*, J. Mason, Ed.; Plenum Press: New York, 1987; p 57.